The American Journal of Pathology, Vol. 180, No. 3, March 2012
Published by Elsevier Inc. on behalf of the
American Society for Investigative Pathology.
DOI: 10.1016/j.ajpath.2011.11.019

Immunopathology and Infectious Diseases

p47^{phox} Directs Murine Macrophage Cell Fate Decisions

Liang Yi,* Qi Liu,* Marlene S. Orandle,†
Sara Sadiq-Ali,* Sherry M. Koontz,* Uimook Choi,‡
Fernando J. Torres-Velez,§ and
Sharon H. Jackson*

From the Molecular Trafficking Unit and the Genetic Immunotherapy Section,‡ Laboratory of Host Defenses, and the Infectious Disease Pathogenesis Section,† Comparative Medicine Branch, National Institute of Allergy and Infectious Diseases, National Institutes of Health, Bethesda, Maryland; and the Foreign Animal Disease Diagnostic Lab,§ Plum Island Animal Disease Center, United States Department of Agriculture, Greenport, New York*

Macrophage differentiation and function are pivotal for cell survival from infection and involve the processing of microenvironmental signals that determine macrophage cell fate decisions to establish appropriate inflammatory balance. NADPH oxidase 2 (Nox2)–deficient chronic granulomatous disease (CGD) mice that lack the gp91^{phox} (gp91$^{phox-/-}$) catalytic subunit show high mortality rates compared with wild-type mice when challenged by infection with *Listeria monocytogenes* (*Lm*), whereas p47^{phox}-deficient (p47$^{phox-/-}$) CGD mice show survival rates that are similar to those of wild-type mice. We demonstrate that such survival results from a skewed macrophage differentiation program in p47$^{phox-/-}$ mice that favors the production of higher levels of alternatively activated macrophages (AAMacs) compared with levels of either wild-type or gp91$^{phox-/-}$ mice. Furthermore, the adoptive transfer of AAMacs from p47$^{phox-/-}$ mice can rescue gp91$^{phox-/-}$ mice during primary *Lm* infection. Key features of the protective function provided by p47$^{phox-/-}$ AAMacs against *Lm* infection are enhanced production of IL-1α and killing of *Lm*. Molecular analysis of this process indicates that p47$^{phox-/-}$ macrophages are hyperresponsive to IL-4 and show higher Stat6 phosphorylation levels and signaling coupled to downstream activation of AAMac transcripts in response to IL-4 stimulation. Notably, restoring p47^{phox} protein expression levels reverts the p47^{phox}-dependent AAMac phenotype. Our results indicate that p47^{phox} is a previously unrecognized regulator for IL-4 signaling pathways that are important for macrophage cell fate choice. ***(Am J Pathol 2012, 180: 1049–1058; DOI: 10.1016/j.ajpath.2011.11.019)***

Activated macrophages maintain inflammatory balance during tissue damage, stress, and immune reactions, and thereby preserve local homeostasis. Inflammation is a protective host response to injury caused by pathological and physiological insults such as microbial infection and tissue damage.[1] It is a biphasic process; involving both vascular and cellular responses, and is triggered by irritants within the local tissue milieu. Macrophages are major innate immune cellular respondents to pathological and physiological environmental signals. Depending on the signal(s) received, macrophages differentiate along classical versus alternative activation pathways. Using this linear categorization, classically activated macrophages are typically defined immunologically as pro-inflammatory mediators, whereas the diverse population of alternatively activated macrophages (AAMac) are classified as anti-inflammatory.[2] However, more recent classification of macrophages based on their homeostatic and regulatory roles such as host defense, wound healing, and immune regulation encompasses their homeostatic as well as immunological function.[3,4] Various innate or adaptive signals initiate CD4$^+$ T-cell activation and differentiation into polarized T helper 1 (T_H1) and T_H2 effectors that secrete cytokines such as interferon (IFN)–γ and interleukin (IL)–4, respectively. In turn, IFN-γ drives classical macrophage activation, whereas IL-4 drives alternative macrophage activation during adaptive immune responses.[5]

We recently reported that p47$^{phox-/-}$ mice,[6] a model of the human immunodeficiency chronic granulomatous disease (CGD), develop AAMac-driven active chronic inflammation[7] characterized by systemic exaggerated chitinase-like Ym1/Ym2 protein[8] secretion and progres-

Supported by the Intramural Research Program of the National Institute of Allergy and Infectious Diseases, NIH and in part by the National Institute on Minority Health and Health Disparities, NIH.

Accepted for publication November 11, 2011.

Supplemental material for this article can be found at *http://ajp.amjpathol.org* or at doi: 10.1016/j.ajpath.2011.11.019.

Address reprint requests to Sharon H. Jackson, M.D., Laboratory of Host Defenses, NIAID, NIH, CRC Bldg 5-West Labs, Room 5–3942, 10 Center Dr MSC 1456, Bethesda, MD 20892-1456. E-mail: sjackson@niaid.nih.gov.

sive crystalline macrophage pneumonia. p47^{phox} is best recognized as an organizing adaptor protein for multicomponent NADPH oxidase (Nox)−2 holoenzyme–dependent superoxide generation.[9,10] Mutations in the genes for p47^{phox} and the membrane-associated catalytic gp91^{phox}/Nox2 subunit comprise the major autosomal recessive and X-linked, respectively, forms of CGD.[11–13] Phagocytes from p47$^{phox-/-}$[6] and gp91$^{phox-/-}$[14] mice are devoid of NADPH oxidase–dependent reactive oxygen species (ROS) production. In addition, similar to human CGD patients, p47$^{phox-/-}$ [6] and gp91$^{phox-/-}$[14] mice develop CGD-like lesions, including those of systemic infection, granulomatous inflammation, and active chronic hyperinflammatory diseases.[13,15,16]

Interestingly p47$^{phox-/-}$ mice spontaneously develop sterile progressive crystalline macrophage pneumonia in a pulmonary niche that also contains high levels of IL-12 and T_H1, T_H2, and T_H17 cytokines.[7] These findings reveal that the sterile spontaneous active chronic inflammation in the p47$^{phox-/-}$ mice is noncanonical, and thereby indicate that there is a more complex basis for the observed aberrant p47$^{phox-/-}$ AAMac-mediated inflammation that is likely to involve contributions from both macrophage intrinsic factors and the inflammatory niche in p47^{phox}-deficient mice.

In this study, we explored the signaling pathways mediating p47$^{phox-/-}$ macrophage default to an AAMac phenotype during primary *Lm* infection. Here we show that AAMacs from p47$^{phox-/-}$ mice provide a protective function against *Listeria monocytogenes* (*Lm*) infection. A key finding is that STAT6 molecular signaling is upregulated and transcription of phenotypic AAMac transcripts is enhanced in p47$^{phox-/-}$ macrophages because the macrophages are hyperresponsive to IL-4 stimulation.

Materials and Methods

Mice

NADPH oxidase p47^{phox}-deficient (p47$^{phox-/-}$) mice have previously been described.[6] The backcrossing of 14 generations with wild-type (WT) C57BL/6NTac generated congenic p47$^{phox-/-}$ mice on a C57BL/6NTac background. Both congenic p47$^{phox-/-}$ and WT control mice (C57BL/6NTac) were obtained from Taconic Farms (Hudson, NY).The p47$^{phox-/-}$ mice were housed in aseptic conditions and given water containing Bactrim (0.13 mg/mL trimethoprim and 0.67 mg/mL sulfamethoxazole; Actiatis MidAtlantic, Columbia, MD). gp91$^{phox-/-}$/Nox2$^{-/-}$ B6.129S6-*Cybb*^{tm1Din}/J mice[14] were obtained from the Jackson Laboratory (Bar Harbor, ME). Nox1$^{-/-}$[17] mice were a generous gift from Dr. Chihiro Yabe-Nishimura (Kyoto Prefectural University of Medicine, Kyoto Japan). All mice were 6 to 8 weeks of age. This study (permit no. ASP LHD 11) was reviewed and approved by the Animal Care and Use Committee of the National Institute of Allergy and Infectious Diseases of the National Institutes of Health (Public Health Service Assurance A4149-01). The study was performed in strict accordance with the recommendations in the Guide for the Care and Use of Laboratory Animals of the National Institutes of Health/National Institute of Allergy and Infectious Diseases.

Bacteria and Reagents

Recombinant *Lm* (rLM-OVA)[18] strain 10403S expressing ovalbumin was a generous gift from Dr. Hao Shen (University of Pennsylvania, School of Medicine, Philadelphia, PA). *Lm* was subcultured on Difco Brain Heart Infusion Agar (BHI; BD, Sparks, MD). Polyethylene glycol SOD (PEG-SOD) was purchased from Sigma-Aldrich (St. Louis, MO), and diphenylene iodonium (DPI) was purchased from Calbiochem (EMD Chemicals, Inc., Gibbstown, NJ).

Histopathology and Immunohistochemistry

Tissue sections (3 to 4 μm) from formalin-fixed paraffin-embedded tissues were stained with hematoxylin and eosin (H&E) and examined for routine histopathology. Similar unstained sections were used for immunofluorescence. For immunofluorescence, slides were deparaffinized in Xylene and rehydrated through graded concentrations of ethanol. A rabbit polyclonal antibody against YM1/YM2 proteins[8] was incubated on the tissue sections at a dilution of 1:250 for 60 minutes at room temperature. The bound YM1/YM2 antibody was detected using a biotinylated anti-rabbit secondary antibody (Vector Labs, Burlingame, CA), followed by streptavidin conjugated with Alexa Fluor 594 (Invitrogen, Carlsbad, CA). For detecting murine macrophage mannose receptor (MMR), sections were incubated with a goat polyclonal antibody against MMR (R&D Systems, Inc., Minneapolis, MN) at a dilution of 1:100 for 60 minutes at room temperature. Bound antibody was detected using a biotinylated anti-goat secondary antibody (Vector Labs), followed by streptavidin conjugated with Alexa Fluor 594 (Invitrogen). Nuclei were stained with DAPI, and sections were mounted with ProLong Gold anti-fade mounting medium (Invitrogen).

Infection of Mice and Determination of Bacterial Load

Overnight rLM-OVA cultures were serially diluted in PBS to the desired dose and injected i.v. into the lateral tail vein or i.p. into the peritoneal cavity of mice as indicated. Inoculates were plated in sterile PBS on BHI agar (BD) to verify dose. Bactrim prophylaxis was discontinued 1 week before infection. Mice were infected with 5×10^4 CFU (0.1 LD_{50}) by i. v. injection. Bacterial loads were determined by plating 10-fold serials dilutions of organ homogenates in sterile PBS on BHI agar (BD).

Macrophage Adoptive Transfer

Donor p47$^{phox-/-}$ mice received 5×10^4 CFU (0.1 LD_{50}) *Lm*. in 1 mL of PBS by i.p. injection, or 1 mL of 3% w/v of thioglycolate 3 days before macrophage harvest. Ten million p47$^{phox-/-}$ inflammatory macrophages were i. v. injected in 10 gp91$^{phox-/-}$ recipient mice 1 day before

Lm infection (as described above). A control group of 10 gp91$^{phox-/-}$ mice received 100 μL of PBS by i.v. injection.

Intracellular Stain and Flow-Cytometric Analysis

Spleens from C57BL/6 WT, p47$^{phox-/-}$ and gp91$^{phox-/-}$ mice infected by 0.1 LD_{50} rLM-OVA were aseptically removed and passed though a nylon mesh screen. Red blood cells were lysed with ACK lysing medium (Lonza, Walkersville, MD). Splenocytes (5×10^6 cells/mL) were resuspended in IMDM complete: IMDM (Gibco/Invitrogen Corp, Carlsbad, CA) containing 10% fetal bovine serum (Hyclone Laboratories, Logan, UT), 2.0 mmol/L L-glutamine (Hyclone), 50 μmol/L β-mercaptoethanol (Sigma Aldrich, St. Louis, MO), and 100 units/mL of penicillin and streptomycin 10 units/mL (Gibco/Invitrogen), and incubated with 10 μg/mL $OVA_{257-264}$ or $OVA_{323-339}$ peptides (synthesized by NIAID Research Technologies Branch- Peptide Synthesis and Analysis Unit, Bethesda, MD). A 1-μg/mL quantity of Golgistop (BD Pharmingen) was added for the final 2 hours of culture. After 5 hours, cells were stained with fluorochrome-labeled antibodies (anti-CD4, anti-CD8, and anti-IL-4; BD Pharmingen, San Diego, CA) using the Cytofix/Cytoperm Kit (BD Pharmingen) according to the manufacturer's instructions. Splenocytes were analyzed on a FACS Canto (BD Bioscience, San Jose, CA), and data were analyzed using FlowJo (Tree Star, Ashland, OR).

Macrophage Preparation and Culture

Peritoneal macrophages were harvested from thioglycolate (Sigma Aldrich, St. Louis, MO)–stimulated mice as previously described.[7] Mice received 2 mL 3% w/v thioglycolate i.p. 3 days before macrophage harvest. Approximately 1×10^6 cells per sample were seeded into 24-well plates in volume of 1 mL. After a 3-hour incubation, the nonadherent cells were removed by washing with PBS. The adherent cells were incubated in DMEM (Gibco/Invitrogen) supplemented with 10% fetal bovine serum (ATCC, Manassas,VA), and stimulated as indicated.

Bone Marrow–Derived Macrophages

Briefly, bone marrow was flushed with PBS, resuspended in 1 mL of ACK lysing medium (Lonza), and incubated at room temperature for 5 minutes to eliminate red blood cells. The single-cell suspension was filtered though a 40-μm cell strainer (BD Falcon/BD Biosciences, San Jose, CA), re-suspended at a density of 3×10^6/mL in complete DMEM (Gibco/Invitrogen) supplemented with 10% fetal bovine serum (ATCC) and 10 ng/mL GM-CSF (R&D Systems), and then plated and incubated in a 5% CO_2 incubator for 5 days. Nonadherent cells were decanted, and the remaining adherent cells were washed with fresh medium and stimulated as indicated.

Lm-*Infected Macrophage Isolation and Culture*

Mice received 5×10^4 CFU (0.1 LD_{50}) *Lm*. in 1 mL of PBS by i.p. injection 7 days before macrophage harvest, as described above.

In Vitro Lm-*Killing Assay*

Bone marrow–derived macrophages were plated on a 24-well plate at 5×10^5 cells per well and cultured with complete DMEM alone or supplemented with IL-4 (1000 U/mL), heat-killed *Lm* (HKL; 1×10^5 CFU/mL), or lipopolysaccharide (100 ng/mL, InvivoGen, San Diego, CA) plus IFN-γ (50 U/mL, R&D Systems) for 24 hours. After washing with PBS, cells were inoculated with 5×10^5 CFU/mL of *Lm* in 1 mL of RPMI 1640 (Gibco/Invitrogen) plus 10% normal mouse serum without antibiotics for 30 minutes. The cells were then incubated with RPMI 1640 plus 10% FCS and 5 μg/mL Gentamicin (Sigma Aldrich) for 30 minutes to kill extracellular bacteria, washed with PBS, and incubated with RPMI 1640 plus 10% fetal calf serum for 5.5 hours (time 6 hours). After 6 hours, the cells were washed and lysed with 0.05% Triton X-100 (Sigma Aldrich). At the 30-minute time point, time 0 cells were washed and lysed with 1 mL of 0.05% Triton X-100 (Sigma Aldrich). The lysates were plated on BHI agar (BD) overnight, and *Lm* killing was determined by counting the number of CFU per well.

Virus Production and Transduction

VSV-G–pseudotyped lentiviral–human p47^{phox} and e-green fluorescent protein (eGFP) were generated by transient cotransfection of the specific transfer vector plasmid with the three packaging plasmids (pMDLg/pRRE, the gag-pol plasmid; pRSV-Rev, a Rev-expressing plasmid; and pMD.G, a VSV-G envelope–expressing plasmid) into 293T cells (ATCC) as described previously.[19] Lentiviral vector supernatant was filtered, concentrated by ultracentrifugation (43,000 $\times$ *g* for 3 hours), and aliquots were stored at -70°C. For transient expression, 20 μL of the concentrated virus was added to the cell culture media, followed by a 30-minute centrifugation (2500 rpm) for 3 consecutive days to enhance the transduction. Transduction was confirmed by microscopic and flow-cytometric detection of eGFP expression using FACS (BD Bioscience).

Quantitative Real-Time PCR

Total RNA was extracted by using the RNeasy Mini Kit (Qiagen, Valencia, CA) according to the manufacturer's instructions. Quantitative real-time PCR (qPCR) was performed with the 7500 Real Time PCR System (Applied Biosystems, Foster City, CA) and performed with 1 ng of RNA samples and specific Gene Expression Assay (Applied Biosystems) using the TaqMan RNA-to-CT 1-Step Kit (Applied Biosystems). The Gene Expression Assays for YM1, Arg1, GAPDH, PKG1, and RPS29 were purchased from Applied Biosystems. The relative change in gene expression was calculated by the $\Delta\Delta$ Ct method

(Applied Biosystems) from triplicate determinations using RPS29 as a reference.

Immunoblotting

Cell lysates were prepared in M-PER Buffer (Pierce Biotechnology, Rockford, IL) supplemented with Halt Protease Inhibitor Cocktail and Phosphatase Inhibitor Cocktail (Pierce Biotechnology). The protein concentrations were determined by the Bradford assay. Proteins were resolved by NuPage 4 to 12% Bis-Tris Gel (Invitrogen, Carlsbad, CA) and transferred to nitrocellulose membranes by iBlot Gel Transfer (Invitrogen). Immunoblotting analyses were performed by SNAPid system (Millipore, Billerica, MA). Immunocomplexes were reacted with Western Blotting Reaction Reagent (GE Healthcare, Piscataway, NJ). Proteins were then visualized by exposed to HyBlot CL film (Denville Scientifics, Metuchen, NJ). Scanned images were analyzed by ImageJ[20] for the relative protein quantification, anti–β-actin monoclonal antibody (Sigma), anti-p47^{phox} polyclonal antibody (Millipore, Billerica, MA), anti–ECF-L monoclonal antibody (R&D Systems), anti-Arg1 monoclonal antibody (BD), anti-phosphorylated Stat6 (pY641) polyclonal antibody (BD) and anti-Stat6 polyclonal antibody (BD) were used as primary antibodies. The secondary antibodies, ECL Mouse IgG, HRP-Linked Whole antibody (from sheep), ECL Rabbit IgG, HRP-Linked Whole antibody (from donkey) and ECL Rat IgG, HRP-Linked Whole antibody (from goat) were purchased from GE Healthcare.

Statistical Analysis

Multigroup test analysis using repeated-measures analysis of variance with the Tukey, Bonferroni, or Newman–Keuls post test using a value of $\alpha = 0.05$ for the 99.9% confidence interval was performed for the real-time PCR and the severity score analyses. Multigroup test analysis using repeated-measures analysis of variance with the Tukey, Bonferroni or Newman–Keuls post test, and two-way analysis of variance with a Bonferroni post test using a value of $\alpha = 0.001$ for the 99.9% confidence interval was performed for the *in vitro* killing assays. Differences between gp91$^{phox-/-}$ recipient mice in the survival analysis were determined by Mantel–Cox log-rank test and the log-rank test for trends (Prism 5; GraphPad Software, San Diego, CA).

Results

p47$^{phox-/-}$ Macrophages Discriminate Classical Versus Alternative Activation Signals

We previously demonstrated that thioglycolate-elicited inflammatory macrophages from p47$^{phox-/-}$ mice discriminate classical versus alternative macrophage activation signals *in vitro*, and that the inflammatory macrophages from the peritoneal cavities of p47$^{phox-/-}$ mice also secrete Ym1 protein *ex vivo*.[7] Using IL-4 to simulate alternative activation or IFN-γ in combination with heat-killed

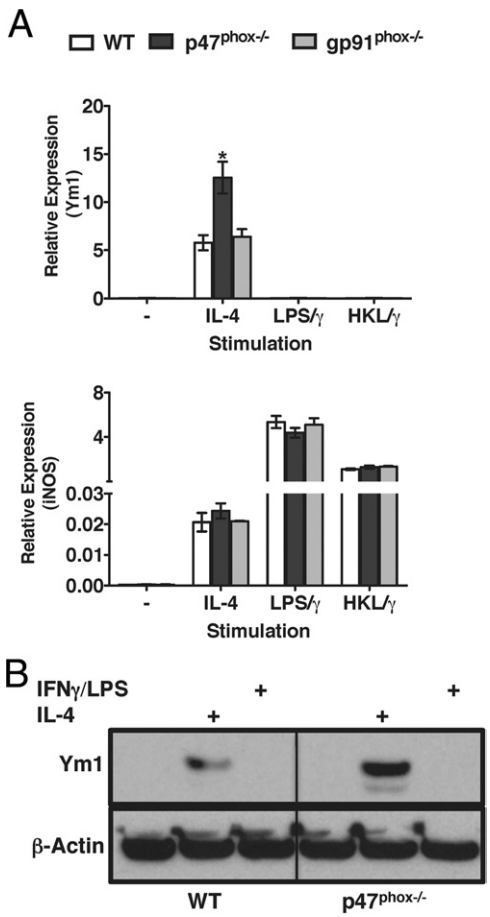

Figure 1. p47$^{phox-/-}$ macrophages discriminate activation signal *in vitro*. Bone marrow–derived macrophages were stimulated overnight with 1000 units/mL IL-4, heat-killed *Lm* (HKL/γ or LPS/γ). **A:** Real-time PCR quantification of Ym1 and iNos. Values are relative to expression of the gene encoding RPS29. Data represent three independent experiments including three to four of each genotype per experiment. *$P < 0.05$. **B:** Total cell lysates from BMMacs stimulated overnight with IL-4 or LPS/γ were blotted with anti-Ym1 or anti–β-actin. Results are representative of two independent experiments including three of each genotype per experiment.

Lm (HKL/γ) or LPS (LPS/γ) to simulate classical activation, we observed that, similar to inflammatory macrophages, bone marrow–derived p47$^{phox-/-}$ macrophages (BMMacs) also discriminate classical versus alternative macrophage activation signals *in vitro* (Figure 1). Using real-time PCR quantification, we found that whereas IL-4 stimulated p47$^{phox-/-}$ BMMacs express more Ym1 than WT or NADPH oxidase 2 catalytic subunit–deficient gp91$^{phox-/-}$ BMMacs, Ym1 gene expression was not detected in WT, p47$^{phox-/-}$ or gp91$^{phox-/-}$ BMMacs treated with classical pathway stimuli (Figure 1A). We also found that, in response to IL-4 as well as classical pathway stimuli, transcription for the classical activation marker iNos was similar in BMMacs from each genotype (Figure 1A).

Protein analysis revealed that neither resting WT nor p47$^{phox-/-}$ BMMacs express Ym1 protein in the absence of *in vitro* stimulation. However, similar to inflammatory p47$^{phox-/-}$ macrophages, IL-4–stimulated p47$^{phox-/-}$ BMMacs express more Ym1 protein than similarly treated WT BMMacs (Figure 1B). These findings indicated that

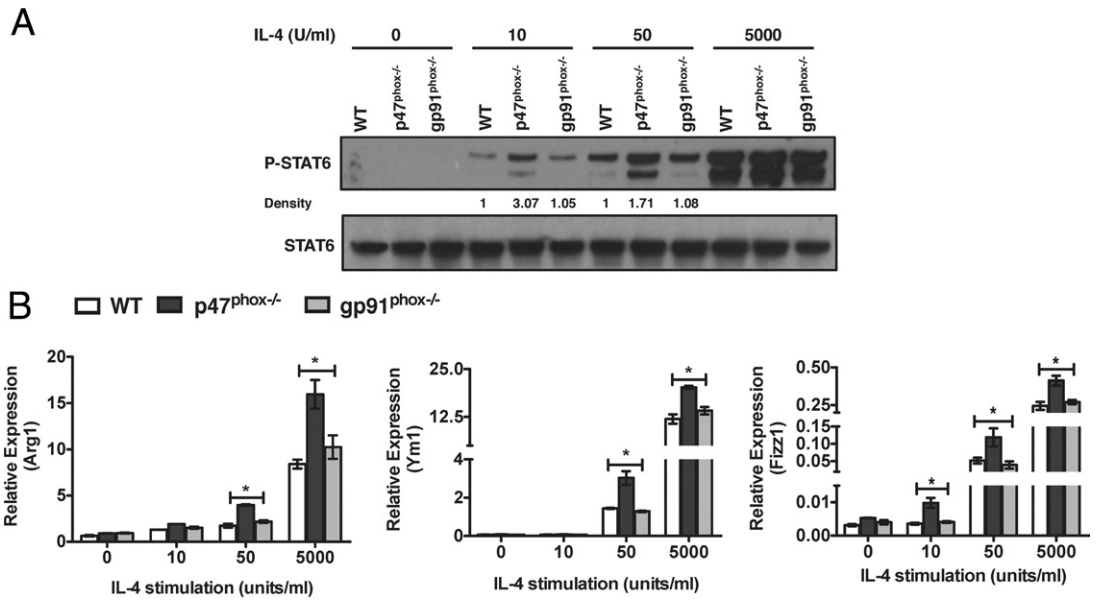

Figure 2. p47^{phox} protein attenuates IL-4 signaling in macrophages independent of the gp91^{phox} catalytic subunit. **A:** Immunoblot analysis of STAT6 phosphorylation in inflammatory macrophages from each genotype stimulated with IL-4 for 20 minutes as indicated. Results of one representative experiment of three independent experiments are shown. **B:** Real-time PCR analysis of Arg1, Ym, and FIZZ1 mRNA from inflammatory macrophages from each genotype stimulated with IL-4 for 18 hours as indicated. Values are relative to expression of the gene encoding RPS29. Data represent three independent experiments including three of each genotype per experiment. $^*P < 0.05$.

although p47$^{phox-/-}$ macrophages discriminated classical versus alternative macrophage activation signals, IL-4 stimulation induced a more robust AAMac phenotype in p47$^{phox-/-}$ macrophages.

p47^{phox} Protein Is Essential for Attenuating IL-4–Dependent Alternative Macrophage Activation

In macrophages, IL-4 induced STAT6 activation, which initiated transcription of specific alternative macrophage activation genes such as Ym1, arginase 1 (Arg1), and FIZZ1.[5] To further discriminate a role for p47^{phox} protein in regulating macrophage cell fate decisions, we next assessed IL-4–induced STAT6 activation, and transcriptional changes in STAT6-regulated AAMac target genes in inflammatory macrophages. Relative to either WT or gp91$^{phox-/-}$ macrophages, STAT6 phosphorylation was significantly enhanced in p47$^{phox-/-}$ macrophages that were treated with 10 and 50 units of IL-4 (Figure 2A). In contrast, there was no difference in STAT6 phosphorylation in WT, p47$^{phox-/-}$, or gp91$^{phox-/-}$ macrophages that were stimulated with a saturating dose of 5000 units of IL-4. Consistent with the finding that Ym1 transcripts are upregulated in IL-4–stimulated p47$^{phox-/-}$ BMMacs relative to similarly treated WT macrophages (Figure 1), transcripts encoding Ym1, Arg1, and FIZZ1 were also upregulated in IL-4–stimulated p47$^{phox-/-}$ inflammatory macrophages (Figure 2B). Interestingly, IL-4–induced transcripts for Ym1, Arg1, and FIZZ1 were similar in WT and gp91$^{phox-/-}$ inflammatory macrophages (Figure 2B). Furthermore, unlike WT or gp91$^{phox-/-}$ macrophages, transcription of FIZZ1 was significantly upregulated in response to 10 units of IL-4 stimulation, and transcripts for FIZZ1, Ym1, and Arg1 were significantly upregulated in response to 50 units of IL-4 stimulation in p47$^{phox-/-}$ macrophages (Figure 2B). These data clearly demonstrate that, unlike WT or gp91$^{phox-/-}$ macrophages, p47$^{phox-/-}$ macrophages are hyperresponsive to IL-4 stimulation, which indicates that the skewed AAMac phenotype is cell intrinsic and due to the loss of p47^{phox} protein expression.

Notably, IL-4 did not trigger STAT6 hyperphosphorylation or enhance transcription of target AAMac genes in gp91$^{phox-/-}$ macrophages *in vitro* (Figure 2). We also found that Ym1 protein expression was similar in IL-4–stimulated macrophages from WT mice, and Nox catalytic subunit gp91^{phox} and Nox1[17]-deficient mice (see Supplemental Figure S1A at *http://ajp.amjpathol.org*). Furthermore, scavenging endogenous superoxide, using the membrane-permeable ROS scavenger polyethylene glycol–superoxide dismutase (PEG-SOD), which converts superoxide into hydrogen peroxide (see Supplemental Figure S1B at *http://ajp.amjpathol.org*), and the selective Nox inhibitor diphenylene iodonium (DPI;[9] see Supplemental Figure S1C at *http://ajp.amjpathol.org*) did not enhance IL-4–induced STAT6 activation in inflammatory WT macrophages. These findings further support the essential role for p47^{phox} protein rather that gp91^{phox}/Nox2 enzymatic activity for regulating IL-4–dependent alternative macrophage activation.

p47$^{phox-/-}$–Dependent AAMac Phenotype Is Rescued by Restoring p47^{phox} Expression

To assess the significance of the p47^{phox} protein for modulating IL-4–dependent alterative macrophage activation, we used a retroviral vector that expresses human

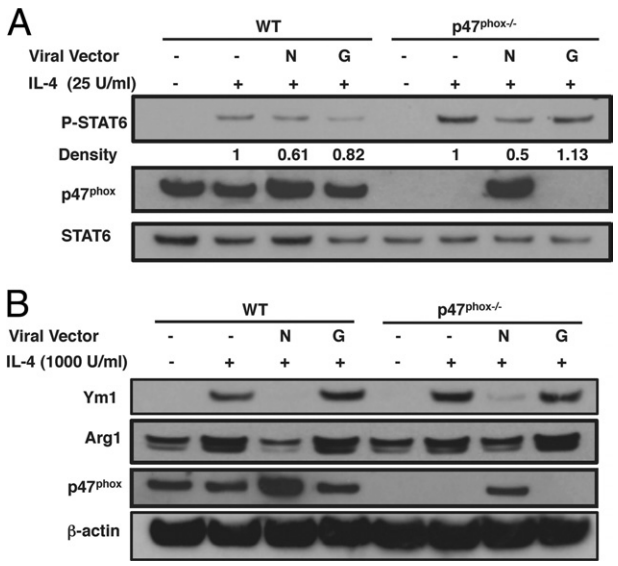

Figure 3. Restoring $p47^{phox}$ protein attenuates signaling downstream of the IL-4R. Immunoblot analysis of $p47^{phox-/-}$ bone marrow–derived macrophages (BMMacs) expressing human $p47^{phox}$ (hNCF1). BMMacs were transduced by viral infection with hNCF1 or control vector (rGFP). **A:** Immunoblot analysis of IL-4–stimulated STAT6 phosphorylation. Quantification relative to total STAT6 is indicated. **B:** Immunoblot analysis of IL-4 stimulated Ym1 and ArgI expression. Results are representative of three independent experiments including three of each genotype per experiment.

$p47^{phox}$ to restore $p47^{phox}$ protein expression in $p47^{phox-/-}$ murine macrophages. Compared with $p47^{phox-/-}$ macrophages transfected with a control vector that expresses green fluorescent protein, when $p47^{phox}$ protein expression was re-established in IL-4–stimulated $p47^{phox-/-}$ macrophages, STAT6 phosphorylation was attenuated (Figure 3A), and Ym1 and Arg1 protein expression were significantly reduced (Figure 3B). Moreover, STAT6 activation was also attenuated (Figure 3A), and Ym1 and Arg1 protein expression were reduced (Figure 3B) in WT macrophages where $p47^{phox}$ is overexpressed. These data support that $p47^{phox}$ protein is necessary and sufficient to revert the WT macrophage phenotype.

Enhanced Lm *Killing by IL-4–Primed* $p47^{phox-/-}$ *Macrophages Is Mediated by IL-1*α

To investigate $p47^{phox-/-}$ macrophage responsiveness *in vivo*, we also assessed macrophage differentiation in $p47^{phox-/-}$ and catalytic subunit $gp91^{phox-/-}$ CGD mice in the context of *Lm* infection.[21] *Lm*, is an intracellular bacterium that induces a robust innate immune response including triggering macrophage NADPH oxidase and nitric oxide–dependent microbial killing; as well as $CD4^+$ T_H1 and $CD8^+$ T lymphocyte IFN-γ–mediated adaptive immunity.[22] Thus, *Lm* infection typically triggers classical macrophage activation and therefore is not expected to induce an AAMac phenotype. We inoculated *Lm* i.p. into WT, $gp91^{phox-/-}$, and $p47^{phox-/-}$ mice and found that the *Lm* bacterial burdens were significantly lower in $p47^{phox-/-}$ peritoneal exudate cells than $gp91^{phox-/-}$ peritoneal exudate cells 3 days postinfection (Figure 4A), which suggests that *Lm* elicited $p47^{phox-/-}$ macrophages have enhanced *Lm* killing. To further investigate the mechanism for the lower *Lm* bacterial load in $p47^{phox-/-}$ *Lm* elicited $p47^{phox-/-}$ macrophages, we next performed *in vitro Lm*-killing assays using BMMacs primed with IFN-γ and heat-killed *Lm* (HKL) to simulate classical macrophage activation, or BMMacs prime with IL-4 to simulate alternative macrophage activation. As expected, we found that the classical pathway induction improved *Lm* killing in both WT and $p47^{phox-/-}$ macrophages. However, we also found that there was significantly more killing of *Lm* in the IL-4–primed $p47^{phox-/-}$ macrophages but not in IL-4–primed WT macrophages (Figure 4B).

We previously reported that although IL-4 induces primarily anti-inflammatory cytokine secretion in WT and $p47^{phox-/-}$ macrophages, both classically and alternatively activated $p47^{phox-/-}$ macrophages hypersecrete IL-1α,[7] which enhances resistance against *Lm* infection.[23] Although the mechanism for the enhanced IL-1α secretion is not yet defined, we speculated that this proinflammatory cytokine secretion might be the basis for the enhanced *Lm* killing in IL-4–primed $p47^{phox-/-}$ macro-

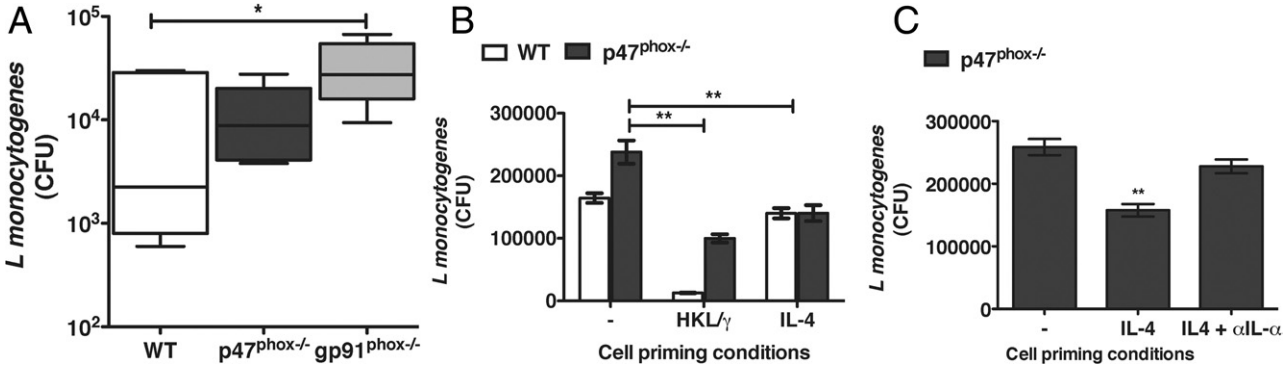

Figure 4. Enhanced *Lm* killing by $p47^{phox-/-}$ AAMacs. Mice were infected with 5×10^4 CFU of *Lm* by i.p. injection. Tissues were harvested 3 days postinfection. **A:** *Lm* peritoneal bacterial burdens 3 days postinfection. Data are mean (± SEM) for six individual mice from two separate experiments with three of each genotype. **B:** *In vitro Lm* killing by WT and $p47^{phox-/-}$ BMMacs primed overnight as indicated, before infection with 5×10^5 CFU *Lm*. Data are mean (± SEM) of seven independent experiments with pooled cells from three of each genotype/experiment. $^{**}P < 0.001$. **C:** *In vitro Lm* killing by $p47^{phox-/-}$ BMMacs primed overnight as indicated, before infection with 5×10^5 CFU *Lm*. Data are mean (± SEM) of three independent experiments with pooled cells from three $p47^{phox-/-}$ mice/experiment. $^{**}P < 0.001$.

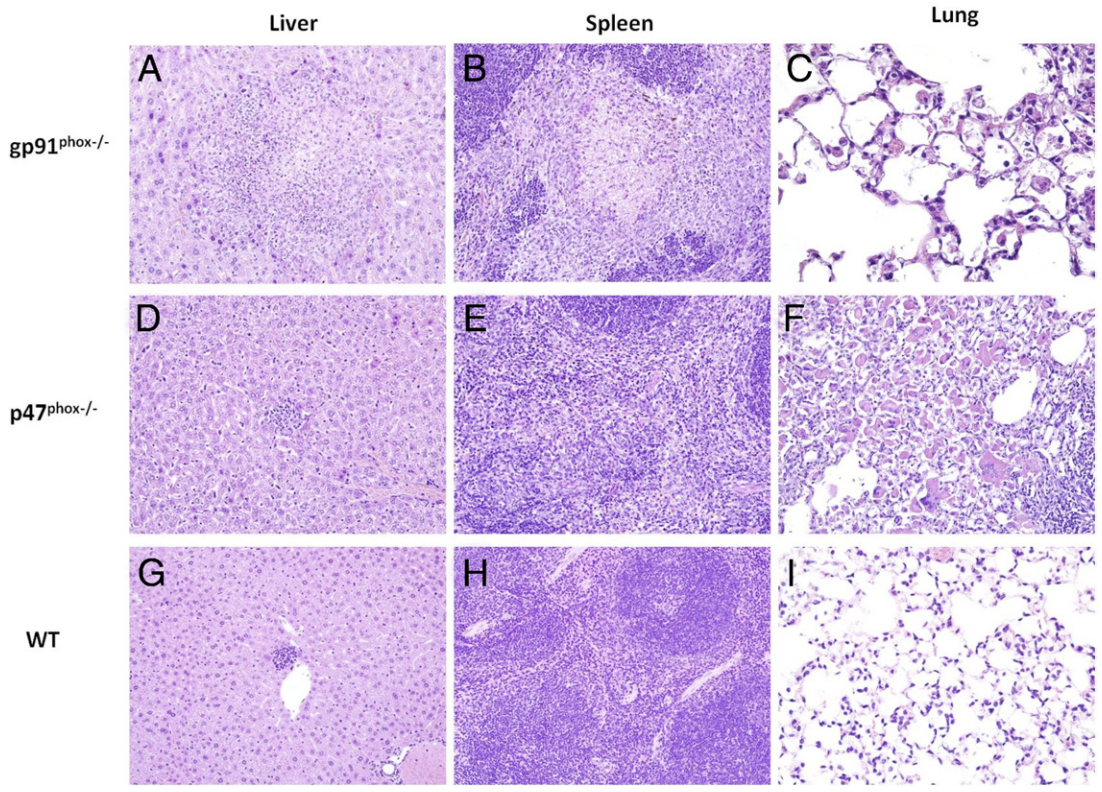

Figure 5. H&E-stained tissue sections from gp91$^{phox-/-}$ (**A–C**), p47$^{phox-/-}$ (**D–F**), and WT (**G–I**) mice showing differences in severity of pathology in multiple tissue types. Changes in the liver and spleen of gp91$^{phox-/-}$ mice at 3 days post-*Lm* infection were more severe than in those of p47$^{phox-/-}$ and WT mice and show evidence of tissue necrosis (original magnification, ×200). Lungs of gp91$^{phox-/-}$ and p47$^{phox-/-}$ contained infiltrates of macrophages and multinucleated giant cells and crystalline pneumonia (original magnification, ×400). Results are representative of five each genotype examined.

phages. In agreement with this hypothesis, we found that the *in vitro* killing by IL-4–treated p47$^{phox-/-}$ macrophages that were also treated with anti–IL-1α antibody before *Lm* infection was similar to that in the untreated p47$^{phox-/-}$ macrophage population (Figure 4C). Thus, blocking the IL-1α activity abolishes the enhanced *in vitro* *Lm* killing demonstrated by IL-4–biased p47$^{phox-/-}$ macrophages, thereby supporting that by secreting IL-1α the p47$^{phox-/-}$ macrophages do kill intracellular *Lm* better than unprimed p47$^{phox-/-}$ macrophages.

p47$^{phox-/-}$ Mice Survive Primary Lm *Infection and Show Less Severe Tissue Pathology*

We next investigated whether p47$^{phox-/-}$ AAMacs would convey protection against *Lm in vivo*. Similar to what we recently reported,[7] p47$^{phox-/-}$ and gp91$^{phox-/-}$ mice developed progressive crystalline macrophage pneumonia 3 days after *Lm* infection (Figure 5). This pneumonia was more severe in p47$^{phox-/-}$ mice when compared with gp91$^{phox-/-}$ mice (Figure 5), and was characterized by intracellular and extracellular accumulation of YM1/YM2-positive crystals (Figure 6A) and intracellular macrophage mannose receptor (Figure 6B), and by increased numbers of alveolar macrophages and multinucleated giant cells. The spleens of gp91$^{phox-/-}$ and p47$^{phox-/-}$ mice were markedly enlarged when compared with *Lm*-infected WT mice, and the white pulp was expanded by infiltrates of macrophages admixed with variable numbers of neutrophils (Figure 5). Splenic inflammation and disruption of the micro-architecture was more extensive and severe in *Lm*-infected gp91$^{phox-/-}$ mice relative to *Lm*-infected WT and p47$^{phox-/-}$ mice 3 days postinfection. In addition, the spleens of *Lm*-infected gp91$^{phox-/-}$ mice contained multiple areas of parenchymal necrosis, which were not evident in either *Lm*-infected WT or p47$^{phox-/-}$ mice. Although spleens from *Lm*-infected p47$^{phox-/-}$ mice were abnormal, livers from these animals were generally unremarkable and contained small scattered foci of inflammation (Figure 5), comparable to what was seen in livers of *Lm*-infected WT mice. In contrast to the mild changes observed in the livers of *Lm*-infected p47$^{phox-/-}$ and WT mice, livers from *Lm*-infected gp91$^{phox-/-}$ showed multiple, often extensive areas of inflammation and necrosis. In gp91$^{phox-/-}$ mice, this severe inflammation and necrosis in both the spleen and liver at 3 days after *Lm* infection was associated with reduced survival (75% versus 100% in p47$^{phox-/-}$ mice).

Our *in vitro* investigations reveal that p47$^{phox-/-}$ macrophages are hyperresponsive to IL-4 stimulation (Figure 2). Therefore, to determine whether the rapid and pronounced AAMac accumulation in *Lm*-infected p47$^{phox-/-}$ tissues was due to aberrant cytokine secretion, we used flow cytometry to assess IL-4 protein expression in T cells from *Lm*-infected mice. As shown in

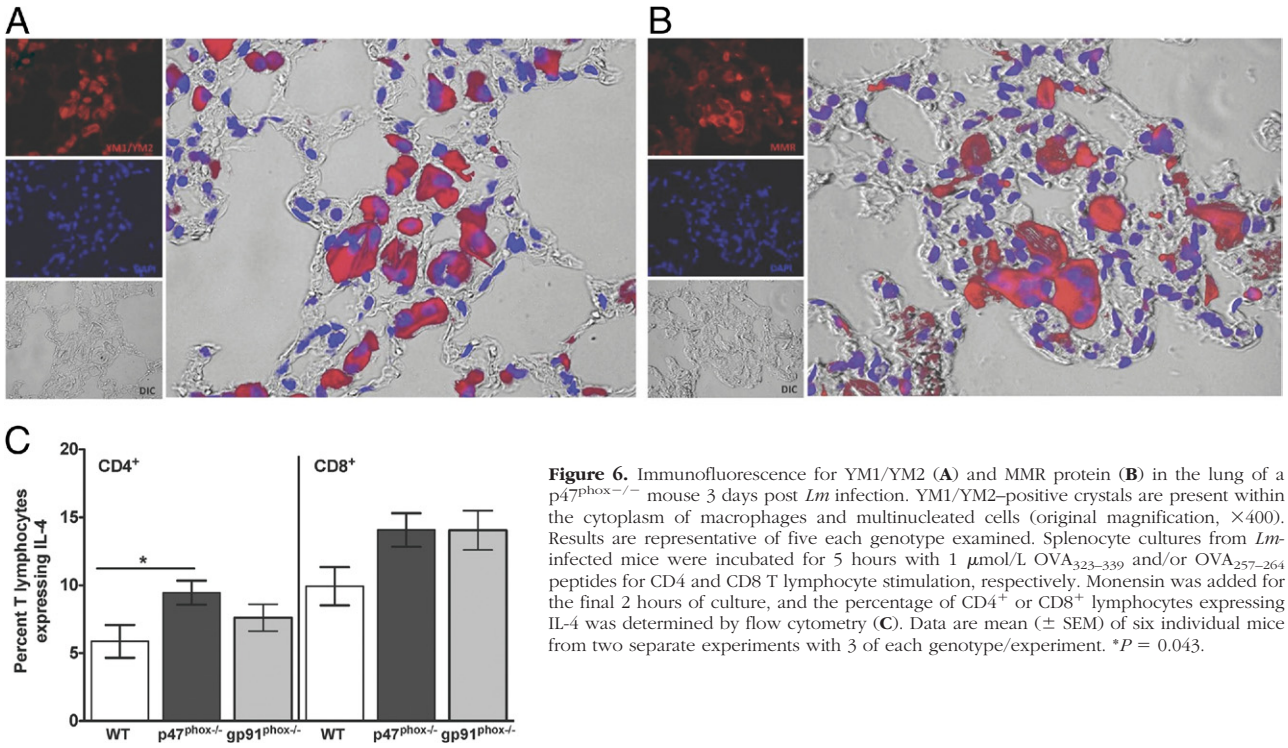

Figure 6. Immunofluorescence for YM1/YM2 (**A**) and MMR protein (**B**) in the lung of a p47$^{phox-/-}$ mouse 3 days post *Lm* infection. YM1/YM2–positive crystals are present within the cytoplasm of macrophages and multinucleated cells (original magnification, ×400). Results are representative of five each genotype examined. Splenocyte cultures from *Lm*-infected mice were incubated for 5 hours with 1 μmol/L $OVA_{323–339}$ and/or $OVA_{257–264}$ peptides for CD4 and CD8 T lymphocyte stimulation, respectively. Monensin was added for the final 2 hours of culture, and the percentage of CD4$^+$ or CD8$^+$ lymphocytes expressing IL-4 was determined by flow cytometry (**C**). Data are mean (± SEM) of six individual mice from two separate experiments with 3 of each genotype/experiment. *P = 0.043.

Figure 6C, the percentage of IL-4–positive CD4$^+$ lymphocytes in the spleens of *Lm*-infected p47$^{phox-/-}$ mice was marginally higher than similarly treated WT T lymphocytes, at 9.5% and 5.9% respectively (P = 0.043). Furthermore, the difference in the percentage of IL-4–positive CD8$^+$ lymphocytes in the *Lm*-infected spleens of WT and p47$^{phox-/-}$ as well as WT and gp91$^{phox-/-}$ mice was not statistically significant (P = 0.057 and P = 0.075, respectively). Thus, these findings indicate that the exaggerated AAMac phenotype in the *Lm*-infected p47$^{phox-/-}$ mice was not driven solely by excessive IL-4 secretion.

Adoptive Transfer of AAMacs from p47$^{phox-/-}$ Mice into Lm*-Infected gp91$^{phox-/-}$ Mice Reduces Tissue Pathology and Enhances Survival*

The finding that p47$^{phox-/-}$ macrophages differentiate into an AAMac phenotype spontaneously in sterile inflammatory lesions[7] and during acute *Lm* infection suggest that selective differentiation along the alternative activation pathway may be advantageous in p47$^{phox-/-}$ mice. To discern whether this is the case in the context of *in vivo Lm* infection, we adoptively transferred *Lm* or thioglycolate elicited inflammatory p47$^{phox-/-}$ macrophages (see *Materials and Methods*) into gp91$^{phox-/-}$ mice before *Lm* infection. All of the recipients of p47$^{phox-/-}$ macrophages survived primary *Lm* infection, compared with 60% of gp91$^{phox-/-}$ mice that were sham injected with PBS before *Lm* infection (Figure 7A). Moreover, gp91$^{phox-/-}$ recipients of p47$^{phox-/-}$ AAMacs showed a reduction in the extent and severity of inflammation and necrosis in both the spleen and liver (Figure 6B). Collectively these observations suggest that AAMacs in *Lm*-infected p47$^{phox-/-}$ mice function to moderate *Lm*-induced disease pathogenesis, particularly with respect to hepatic

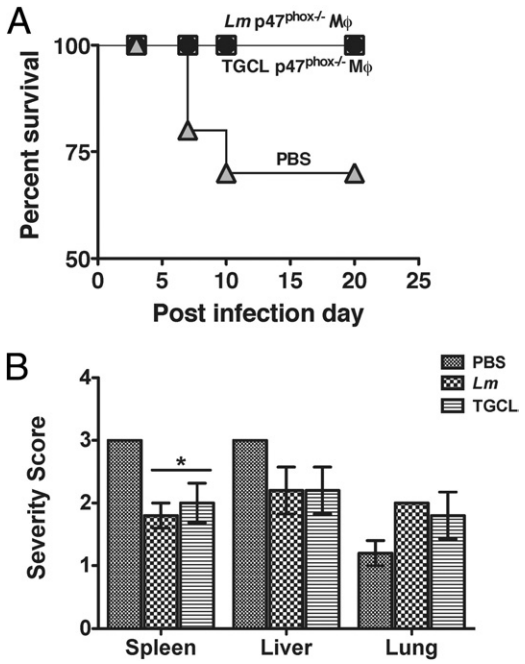

Figure 7. Enhanced survival of gp91$^{phox-/-}$ mouse recipients of p47$^{phox-/-}$ AAMacs. **A:** gp91$^{phox-/-}$ Mouse survival after adoptive transfer of 10 × 10^6 *Lm* or thioglycolate (TGCL)) elicited p47$^{phox-/-}$ inflammatory macrophages before *Lm* infection. PBS indicates survival of gp91$^{phox-/-}$ control recipients that received PBS by i.v. injection. n = 10 per group. P = 0.048. **B:** Tissue severity scores for gp91$^{phox-/-}$ recipients of *Lm* or TGCL elicited p47$^{phox-/-}$ inflammatory macrophages. n = 5 per group. *P < 0.05.

and splenic necrosis, thereby enhancing survival in these mice.

Discussion

A physiological aim of inflammation is to restore tissue homeostasis.[1] However, cancer, autoimmunity, and active inflammatory disease in immunodeficiency each pose distinct tissue insults that drive chronic inflammation that is not restorative. Furthermore, persistent insults can alter the function of inflammatory mediators and effectors, which include macrophages and T cells. During cell-mediated immune responses, T_H1-derived IFN-γ and pathogen recognition receptor activation prime macrophages to become classically activated. These macrophages produce reactive oxygen and nitrogen intermediates to facilitate their microbicidal function, secrete pro-inflammatory cytokines, and can be tumoricidal.[3,5] In contrast, T_H2-driven pathogenesis and T_H2-derived IL-4 and/or IL-13 adaptive immune responses, and local tissue injury, induce alternative macrophage activation. These macrophages promote wound healing and inhibit pro-inflammatory cytokine production.[3,5] We also show, for what we believe is the first time, that $p47^{phox-/-}$ and $gp91^{phox-/-}$ CGD mice develop distinct acute, innate cellular responses and granulomatous inflammation in response to *Lm* infection. Although both *Lm*-infected CGD mice develop granulomatous inflammation, the extent and severity of pathology observed differ between the two strains. We show that during acute primary *Lm* infection, $gp91^{phox-/-}$ mice develop an aggressive granulomatous influx with necrotizing lesions in the liver and spleen, whereas *Lm*-infected $p47^{phox-/-}$ mice develop less severe granulomatous inflammation in lung and spleen, without evidence of necrosis.

Abscess and granuloma formation are characteristic CGD defense reactions to infection with pathogens that are typically eliminated by ROS. In addition, both lesions cause local tissue injury. However, our investigations reveal that the CGD knockout mouse inflammatory response to acute sublethal *Lm* infection is different. Although the acute granulomatous lesions in the $p47^{phox-/-}$ mice accumulate large numbers of $Ym1^+$ AAMacs, the $gp91^{phox-/-}$ mouse lesions are more typical of those seen in IFN-γ– and tumor necrosis factor–α–driven suppurative granulomas that are a hallmark of chronic *Lm* infection.[24–26] The finding of such dramatically disparate acute tissue reactions in the CGD mice strongly suggests that there is a cell-intrinsic basis for the observed enhanced AAMac differentiation in $p47^{phox-/-}$ macrophages. Indeed, we discerned that unlike WT or $gp91^{phox-/-}$ macrophages, $p47^{phox-/-}$ macrophages are hyperresponsive to IL-4 stimulation. Relative to both WT and $gp91^{phox-/-}$ macrophages, STAT6 activation and STAT6 specific transcripts were significantly upregulated in $p47^{phox-/-}$ macrophages at lower doses of IL-4. Moreover, restoring $p47^{phox}$ protein function corrected the aberrant IL-4 driven $p47^{phox-/-}$ AAMac phenotype, which suggests that $p47^{phox}$ protein regulates IL-4 signaling upstream of STAT6 activation.

Potential regulatory mechanisms for $p47^{phox}$ protein upstream of STAT6 are not entirely clear. A previous report showed an association between $p47^{phox}$ and the IL-4R α in Epstein–Barr virus–transformed human B cells.[27] Interestingly, preliminary investigations revealed that $p47^{phox}$ co-immunoprecipitates with the IL-4R-α in Raw264 monocyte-macrophage cells. Therefore, future studies will be extended to primary macrophages once high-affinity antibodies are available for comprehensive analyses of IL-4–induced protein–protein interactions that involve the $p47^{phox}$ protein.

CGD is a multifaceted clinical disease and a unique model of host immune defense. The genetically engineered murine models of the most common genetic variants of CGD[6,14] each recapitulate that the phagocyte respiratory burst is critical for combating microbial infection. Furthermore, these models allow complex analyses of innate and adaptive immune responses that are not possible in human CGD patients. In addition, the murine model can also be used to assess whether $p47^{phox}$, the essential adaptor protein for Nox2-dependent ROS activity, functions independently of the catalytic $gp91^{phox}$/Nox2 subunit, and to investigate clinical consequences of $p47^{phox}$ protein deficiency. Although it has been reported that IL-4 induced Nox1 and Nox5-dependent ROS,[28] our investigations showed that STAT6 activation and target transcripts are similar in IL-4–stimulated WT and $gp91^{phox-/-}$ macrophages. In addition, neither $gp91^{phox-/-}$ nor Nox1-deficient macrophages hyperproduced signature AAMac proteins in response to IL-4 stimulation, as observed in $p47^{phox-/-}$ macrophages. Collectively, these findings indicate that $p47^{phox}$ works independent of the $gp91^{phox}$/Nox2 catalytic subunit to attenuate IL-4–stimulated macrophage activation. Consistent with our observations, recent investigations have revealed that, independent of its role in generating Nox2-dependent ROS, $p47^{phox}$ is an important protein for integrating signaling downstream of TLR9 in murine dendritic cells.[29]

Granulomas are organized microenvironments that provide physical barriers to contain pathogens that escape from macrophages that are incompetent because of protein dysfunction or microbial manipulation. Although granulomas are controlled inflammatory sites, they are also dynamic structures composed of active effector cells that also cause tissue injury. An early, innate response to tissue injury is mast cell– and basophil-derived IL-4 production,[3,30] which could drive the AAMac differentiation observed in both CGD mice during acute *Lm* infection, albeit by different mechanisms. The AAMac phenotype in *Lm*-infected $gp91^{phox-/-}$ mice could be explained by tissue IL-4 production in response to extensive tissue damage and necrosis. In contrast, although there is a relative lack of tissue necrosis in *Lm*-infected $p47^{phox-/-}$ mice, consistent with the CGD phenotype, these mice develop abscesses that cause tissue injury and can thereby trigger local IL-4 production. Therefore, the exaggerated AAMac phenotype in *Lm*-infected $p47^{phox-/-}$ mice could be explained by the $p47^{phox-/-}$ macrophage predisposition to hyperrespond to IL-4 produced in the damaged tissues.

Our original report of the p47$^{phox-/-}$ mice showed that they could develop severe, spontaneous systemic infection with granulomatous inflammation. Furthermore, we also reported that the tissues from the spontaneous lesion in the p47$^{phox-/-}$ mice contained variable amounts of granuloma, abscess, and infection.[6] Subsequently, we demonstrated that these mice developed granulomatous inflammation without infection.[7] In this report, using a controlled acute infection model, we now show that with low-level bacterial stimulation, during the acute phase of *Lm* infection, the p47$^{phox-/-}$ mice develop granulomatous inflammation with AAMacs. In addition, our current findings suggest that these AAMacs also convey a relative protection. In conclusion, using histological analysis as well as *ex vivo* molecular and cellular investigations, we report a novel mechanism by which p47$^{phox-/-}$ mice develop extensive, systemic alternative macrophage activation. These findings allow broader speculation about the basis for the nonrestorative chronic inflammation that is observed in CGD patients, and may explain why clinical disease in X-linked CGD patients can be more severe than in autosomal recessive CGD patients.[16]

Acknowledgments

We thank Kevin Gardner for helpful discussions and critique of this manuscript. We also thank Sharon Wahl, Harry Malech, and Warren Strober for careful review and critique of this manuscript.

References

1. Medzhitov R: Origin and physiological roles of inflammation. Nature 2008, 454:428–435
2. Gordon S, Taylor PR: Monocyte and macrophage heterogeneity. Nat Rev Immunol 2005, 5:953–964
3. Mosser DM, Edwards JP: Exploring the full spectrum of macrophage activation. Nat Rev Immunol 2008, 8:958–969
4. Stout RD, Watkins SK, Suttles J: Functional plasticity of macrophages: in situ reprogramming of tumor-associated macrophages. J Leukoc Biol 2009, 86:1105–1109
5. Gordon S, Martinez FO: Alternative activation of macrophages: mechanism and functions. Immunity 2010, 32:593–604
6. Jackson SH, Gallin JI, Holland SM: The p47phox mouse knock-out model of chronic granulomatous disease. J Exp Med 1995, 182:751–758
7. Liu Q, Cheng LI, Yi L, Zhu N, Wood A, Changpriroa CM, Ward JM, Jackson SH: p47phox Deficiency induces macrophage dysfunction resulting in progressive crystalline macrophage pneumonia. Am J Pathol 2009, 174:153–163
8. Ward JM, Yoon M, Anver MR, Haines DC, Kudo G, Gonzalez FJ, Kimura S: Hyalinosis and Ym1/Ym2 gene expression in the stomach and respiratory tract of 129S4/SvJae and wild-type and CYP1A2-null B6, 129 mice. Am J Pathol 2001, 158:323–332
9. Bedard K, Krause KH: The NOX family of ROS-generating NADPH oxidases: physiology and pathophysiology. Physiol Rev 2007, 87: 245–313
10. El-Benna J, Dang PM, Gougerot-Pocidalo MA, Marie JC, Braut-Boucher F: p47phox, the Phagocyte NADPH oxidase/NOX2 organizer: structure, phosphorylation and implication in diseases. Exp Mol Med 2009, 41:217–225
11. Clark RA, Malech HL, Gallin JI, Nunoi H, Volpp BD, Pearson DW, Nauseef WM, Curnutte JT: Genetic variants of chronic granulomatous disease: prevalence of deficiencies of two cytosolic components of the NADPH oxidase system. N Engl J Med 1989, 321:647–652
12. Roos D: The genetic basis of chronic granulomatous disease. Immunol Rev 1994, 138:121–157
13. Stasia MJ, Li XJ: Genetics and immunopathology of chronic granulomatous disease. Semin Immunopathol 2008, 30:209–235
14. Pollock JD, Williams DA, Gifford MA, Li LL, Du X, Fisherman J, Orkin SH, Doerschuk CM, Dinauer MC: Mouse model of X-linked chronic granulomatous disease, an inherited defect in phagocyte superoxide production. Nat Genet 1995, 9:202–209
15. Schappi MG, Jaquet V, Belli DC, Krause KH: Hyperinflammation in chronic granulomatous disease and anti-inflammatory role of the phagocyte NADPH oxidase. Semin Immunopathol 2008, 30:255–271
16. Rosenzweig SD: Inflammatory manifestations in chronic granulomatous disease (CGD). J Clin Immunol 2008, 28 Suppl 1:S67–72
17. Matsuno K, Yamada H, Iwata K, Jin D, Katsuyama M, Matsuki M, Takai S, Yamanishi K, Miyazaki M, Matsubara H, Yabe-Nishimura C: Nox1 is involved in angiotensin II-mediated hypertension: a study in Nox1-deficient mice. Circulation 2005, 112:2677–2685
18. Foulds KE, Rotte MJ, Seder RA: IL-10 is required for optimal CD8 T cell memory following Listeria monocytogenes infection. J Immunol 2006, 177:2565–2574
19. Dull T, Zufferey R, Kelly M, Mandel RJ, Nguyen M, Trono D, Naldini L: A third-generation lentivirus vector with a conditional packaging system. J Virol 1998, 72:8463–8471
20. Rasband WS: ImageJ, U. S. National Institutes of Health, Bethesda, MD, 1997–2011
21. Mackaness GB: Cellular resistance to infection. J Exp Med 1962, 116:381–406
22. Pamer EG: Immune responses to Listeria monocytogenes. Nat Rev Immunol 2004, 4:812–823
23. Rogers HW, Sheehan KC, Brunt LM, Dower SK, Unanue ER, Schreiber RD: Interleukin 1 participates in the development of anti-Listeria responses in normal and SCID mice. Proc Natl Acad Sci USA 1992, 89:1011–1015
24. Popov A, Abdullah Z, Wickenhauser C, Saric T, Driesen J, Hanisch FG, Domann E, Raven EL, Dehus O, Hermann C, Eggle D, Debey S, Chakraborty T, Kronke M, Utermohlen O, Schultze JL: Indoleamine 2,3-dioxygenase-expressing dendritic cells form suppurative granulomas following Listeria monocytogenes infection. J Clin Invest 2006, 116:3160–3170
25. Vazquez-Boland JA, Kuhn M, Berche P, Chakraborty T, Dominguez-Bernal G, Goebel W, Gonzalez-Zorn B, Wehland J, Kreft J: Listeria pathogenesis and molecular virulence determinants. Clin Microbiol Rev 2001, 14:584–640
26. Mielke ME, Peters C, Hahn H: Cytokines in the induction and expression of T-cell-mediated granuloma formation and protection in the murine model of listeriosis. Immunol Rev 1997, 158:79–93
27. Izuhara K, Arinobu Y, Sumimoto H, Nunoi H, Takeya R, Higuchi K, Takeshige K, Hamasaki N, Harada N: Association of the interleukin-4 receptor alpha chain with p47phox, an activator of the phagocyte NADPH oxidase in B cells. Mol Immunol 1999, 36:45–52
28. Sharma P, Chakraborty R, Wang L, Min B, Tremblay ML, Kawahara T, Lambeth JD, Haque SJ: Redox regulation of interleukin-4 signaling. Immunity 2008, 29:551–564
29. Richter C, Juan MH, Will J, Brandes RP, Kalinke U, Akira S, Pfeilschifter JM, Hultqvist M, Holmdahl R, Radeke HH: Ncf1 provides a reactive oxygen species-independent negative feedback regulation of TLR9-induced IL-12p70 in murine dendritic cells. J Immunol 2009, 182:4183–4191
30. Loke P, Gallagher I, Nair MG, Zang X, Brombacher F, Mohrs M, Allison JP, Allen JE: Alternative activation is an innate response to injury that requires CD4+ T cells to be sustained during chronic infection. J Immunol 2007, 179:3926–3936